Effect of Annealing Temperature on Structural, Morphological, Optical and Magnetic Properties of $NiFe_2O_4$ Thin Films

Original Paper Published: 18 January 2018

Volume 31, pages 2949–2958, (2018) Cite this article

Journal of Superconductivity and Novel Magnetism

Aims and scope

Submit manuscript

Apparao R. Chavan, Rahul R. Chilwar, Prashant B. Kharat & K. M. Jadhav

Abstract

Nickel ferrite ($NiFe_2O_4$) thin films have been deposited on glass substrates by a chemical spray pyrolysis technique at 350 \(^{\circ }\)C substrate temperature. The deposited films were annealed at four different temperatures (400, 450, 500 and 550 \(^{\circ }\)C), and the effect of annealing temperature on the structural, morphological, optical and magnetic properties

were studied. The annealed films were characterized by X-ray diffraction (XRD), Fourier transform infrared spectroscopy (FT-IR), field emission scanning electron microscopy (FE-SEM), UV-visible spectroscopic analysis and vibrating sample magnetometer (VSM). XRD patterns showed that the $NiFe_2O_4$ is oriented along (311) plane, which enhances peak intensity with respect to the annealing temperature. The analysis of XRD pattern revealed the formation of single-phase cubic spinel structure. The FT-IR spectrum of $NiFe_2O_4$ thin films showed strong absorption peaks around 616 and 353 cm^{-1} which indicates the cubic spinel crystal structure of the films. FE-SEM micrographs show that the grain size increases with an increase in annealing temperature. The grain size varies between \(\sim \) 19 and \(\sim \) 28 nm, confirming the nanocrystalline nature of the prepared thin films. The optical properties of the films were studied by an absorbance spectrum in the range of 300 to 800 nm. The results showed that the energy band gap decreased with the increase of annealing temperature. Magnetic properties of $NiFe_2O_4$ thin films exhibit a strong dependence on the annealing temperature. The saturation magnetization increases from \(\sim \) 68.29 to \(\sim \) 205.24 emu/cm^3 with increasing annealing temperature, which is in favour of modern electronic device miniaturization.

1 Introduction

Ferrite thin films are attractive materials because of their useful electrical and magnetic properties, high chemical stability and mechanical hardness [1, 2]. On the basis of their properties, ferrite thin films have applications in many fields such as magnetic recording media, microwave devices, gas sensors, transformers, magnetic core of coils and ferrofluid, switch mode power supplies, deflection of yoke rings and spintronic devices [3,4,5,6]. Several researchers have studied ferrite thin films prepared by different techniques for different applications. In recent years, considerable attention has been focused to the nanostructured spinel ferrite thin films because of their different properties from the bulk material [7]. Thin films are a suitable type of nanostructure which finds many applications. Since decade, because of novel magnetic properties with reduced dimensions, a myriad of research activities in the synthesis and characterization of ferrite nanostructures has been undertaken by many researchers. Spinel ferrite (MFe_2O_4 where 'M' is transition metal) nanostructures have been widely explored in the literature for various applications. In normal spinel ferrites, the M^{2+} cations exclusively occupy the tetrahedral sites, whereas in the inverse ferrites, they are located on the octahedral site, and the tetrahedral position is occupied by half of the Fe^{3+} ions [8]. On account of remarkable structural, electrical and magnetic properties, spinel ferrites are widely used in electronic devices. However, these properties are observed to depend on the deposition conditions [9]. It can be possible to control the properties of thin films by varying the deposition conditions and annealing temperature. There are various growth parameters that affect the microstructure of the thin film such as annealing temperature during deposition and lattice mismatch between the film and substrate. Surface and size effects lead to strong deviations from bulk properties. Surface and size effects depend on the annealing temperature of the sample and stoichiometry [10].

Scheme 1

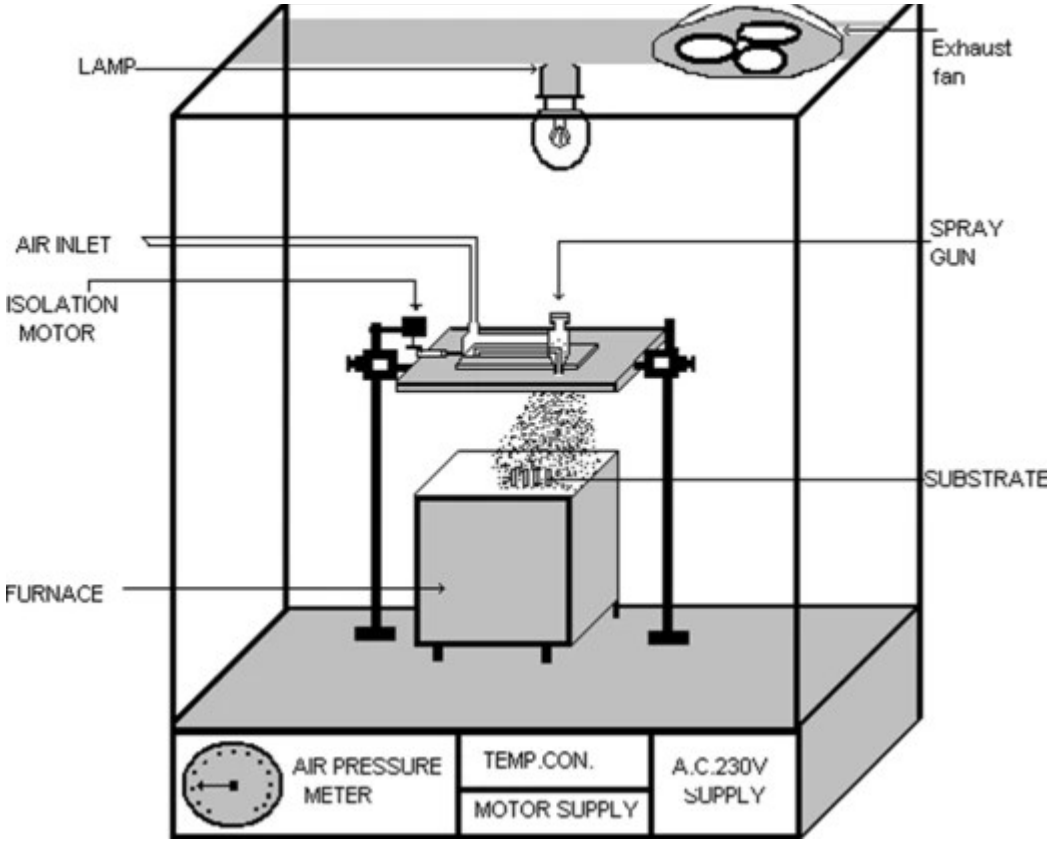

Spray pyrolysis technique

Among all the ferrite materials, a spinel-type nickel ferrite ($NiFe_2O_4$) is one of the most versatile and technologically important ferrites because of its typical ferromagnetic properties, low conductivity and thus lower eddy current losses, high electrochemical stability, catalytic behaviour and abundance in nature [11]. $NiFe_2O_4$ is the most suitable material for device applications in the upper microwave and lower millimetre wave ranges. It can be crystallized is inverse spinel structure; i.e. tetrahedral sites are occupied by ferric ions and the octahedral sites by ferric and nickel ions. The polycrystalline morphology with large grain size leads to a low signal-to-noise ratio [12]. Nickel ferrite ($NiFe_2O_4$) has been widely studied as a magnetic material and considered as a gas sensor in the bulk form towards chlorine, hydrogen sulfide, acetone and LPG [13]. There are a number of deposition techniques available for thin films, such as pulsed laser deposition (PLD) [14], r.f. sputtering [15], ferrite platting [16], dip coating processes [17], electrodeposition [18] and spray pyrolysis [19]. The spray pyrolysis method is widely used due to its simplicity, cheapness and usefulness for the preparation of ferrite film with a large area. Some advantages of the spray pyrolysis technique is a large area of deposited film, low energy for the preparation, easy coating and control of the

thickness of the film [20]. This method has the production capability of highly mixed thin films with two or more compounds since their initial compounds are mixed in solution form. Furthermore, doping is easily done with a very accurate percentage of raw materials. Using this method, controllable size, uniform distribution of grain size, etc., can be achieved [21]. No systematic investigations on structural, morphological, infrared and optical properties of nickel ferrite films deposited (at temperature 350 \(^{\circ }\)C) by a spray pyrolysis technique and annealed at 400, 450, 500 and 550 \(^{\circ }\)C were observed in the literature. In the present work, $NiFe_2O_4$ thin films were deposited using the spray pyrolysis technique and the deposited films were annealed at different temperatures. As observed from the literature, few reports are available on the synthesis of $NiFe_2O_4$ thin films using a spray pyrolysis system and the effect of annealing temperature on structural, morphological, magnetic and optical properties [22, 23].

2 Experimental Details

2.1 Synthesis of Nickel Ferrite Thin Films

The nickel ferrite thin films were deposited onto the preheated glass substrates using a simple chemical spray pyrolysis technique. The spraying solution was sprayed onto preheated glass substrates at different quantities of spraying solutions at an interval of 10 mL. The film was deposited by optimizing various parameters. The substrate temperature was kept around 350 \(^{\circ }\)C. Before depositing the film, the glass substrates were dipped in chromic acid for 30 min. Further, the glass substrates were cleaned by an ultrasonication process for 20 min in distilled water and dried in the air.

Iron nitrate ($Fe(NO_3)_3 \cdot 9H_2O$) and nickel nitrate ($Ni(NO_3)_2 \cdot 6H_2O$) obtained from Merck were dissolved in distilled water with the desired molar ratio 0.08 and volumetric ratio 1:2. The prepared solution was atomized on a glass substrate via a pneumatic spray system under the air pressure 0.25 MPa using a step-by-step film growth. The cleaned glass substrate was mounted on the surface of the hot plate, and the substrate temperature was set to 350 \(^{\circ }\)C. The temperature controller was used to control the temperature within \(\pm \) 10 °C through a thermocouple connected to the surface of a hot plate. The optimizing parameters like nozzle distance to the substrate and air pressure are given in Table 1.

Compressed air was used as a carrier gas to atomize the spray. The atomized droplets were transferred onto the heated glass substrate for 10 s intermittently. The chemical formation of nickel ferrite can be expressed as the following reaction:

$$\begin{array}{@{}rcl@{}} &&\text{Ni}\left({\text{NO}_{\text{3}}} \right)_{\text{2}} \!\cdot\! \text{6H}_{\text{2}} \mathrm{O}+\text{2Fe}\left({\text{NO}_{\text{3}}} \right)_{\text{3}} \!\cdot\! \text{9H}_{\text{2}} \mathrm{O}\,+\,\text{2O}_{\text{2}} \!\to\! \text{NiFe}_{\text{2}} \mathrm{O}_{\text{4}}\\ &&~\,+\,\left({\text{NO}_{\text{3}}} \right)_{\text{2}} \uparrow \,+\,\left({\text{NO}_{\text{3}}} \right)_{\text{3}} \uparrow \!+\text{6H}_{\text{2}} \mathrm{O}+\!\uparrow \text{9H}_{\text{2}} \mathrm{O}\uparrow \end{array} $$

Before the characterization, thin film was annealed at different temperatures, viz. 400, 450, 500 and 550 \(^{\circ }\)C, in a furnace at ambient atmosphere for 4 h. Scheme 1 shows the experimental setup of spray pyrolysis technique.

Table 1 Experimental parameters of $NiFe_2O_4$ thin films by a spray pyrolysis deposition process

2.2 Characterizations

The structural properties of $NiFe_2O_4$ thin films were studied by using a Bruker D8 Advance X-ray powder diffractometer with Cu-Kα (λ= 1.5406 Å) radiations. The surface morphology of the films was investigated using a Brucker S-4800 (Japan) field emission scanning electron microscope. The FT-IR spectrum was recorded using a PerkinElmer infrared spectrometer (model 783) in the range 350–4000 cm^{-1}. The optical properties of the thin films were measured by using a UV-vis spectrophotometer (PerkinElmer Lambda 950). Magnetic properties of the films were measured with a vibrating sample magnetometer (Lakeshore VSM 7410) at room temperature.

3 Results and Discussion

3.1 X-ray Diffraction

Figure 1 shows the X-ray diffraction (XRD) pattern of as-deposited and annealed $NiFe_2O_4$ thin films. The deposited (350 °C) thin film did not show any distinct diffraction peak, but broad peak shows that the film is amorphous in nature. The annealed $NiFe_2O_4$ film is oriented along (311) plane, and other orientations corresponding to (220), (400), (411), (422), (510) and (440) planes are also present with low relative intensities compared to that of (311) plane. The intensity of these planes increases with an increase in annealing temperature. It can be seen that all the annealed films exhibit a spinel cubic crystal structure. The film crystallinity increases with annealing temperature which has been found to be at a maximum of 550 \(^{\circ }\)C. From using the XRD data, the lattice constant and other structural parameters were calculated. The value of lattice parameter increases from 8.2378 to 8.4437 Å and obeys Vegard's rule [24]. The average crystalline size (D) was calculated by using Scherrer's formula [25]

$$ D=\frac{0.9\lambda} {\beta \cos \theta} $$

(1)

where \(\lambda \) is the wavelength of X-ray (1.5406 Å), \(\beta \) is the full width at half maximum in radians and \(\theta \) is the angle of diffraction. The crystallite size increases from 6 to 11 nm. It can be seen that lattice parameter and crystallite size increase with an increase in annealing temperature as shown in Fig. 2. The X-ray density (d_X) is estimated by the following formula [26]:

$$ d_{\mathrm{X}} =\frac{8M}{Na^{3}} $$

(2)

where M is the molecular weight, N is Avogadro's number and \(\alpha \) is the lattice constant. The X-ray density decreases with increasing annealing temperature. The lattice constant, X-ray density and crystallite size are tabulated in Table 2 with different annealing temparatures. The increase in lattice parameter with annealing temperature is due to the strain developed in the films. The obtained results on structural studies are in consistent with

those reported in the literature [22].

Fig. 1

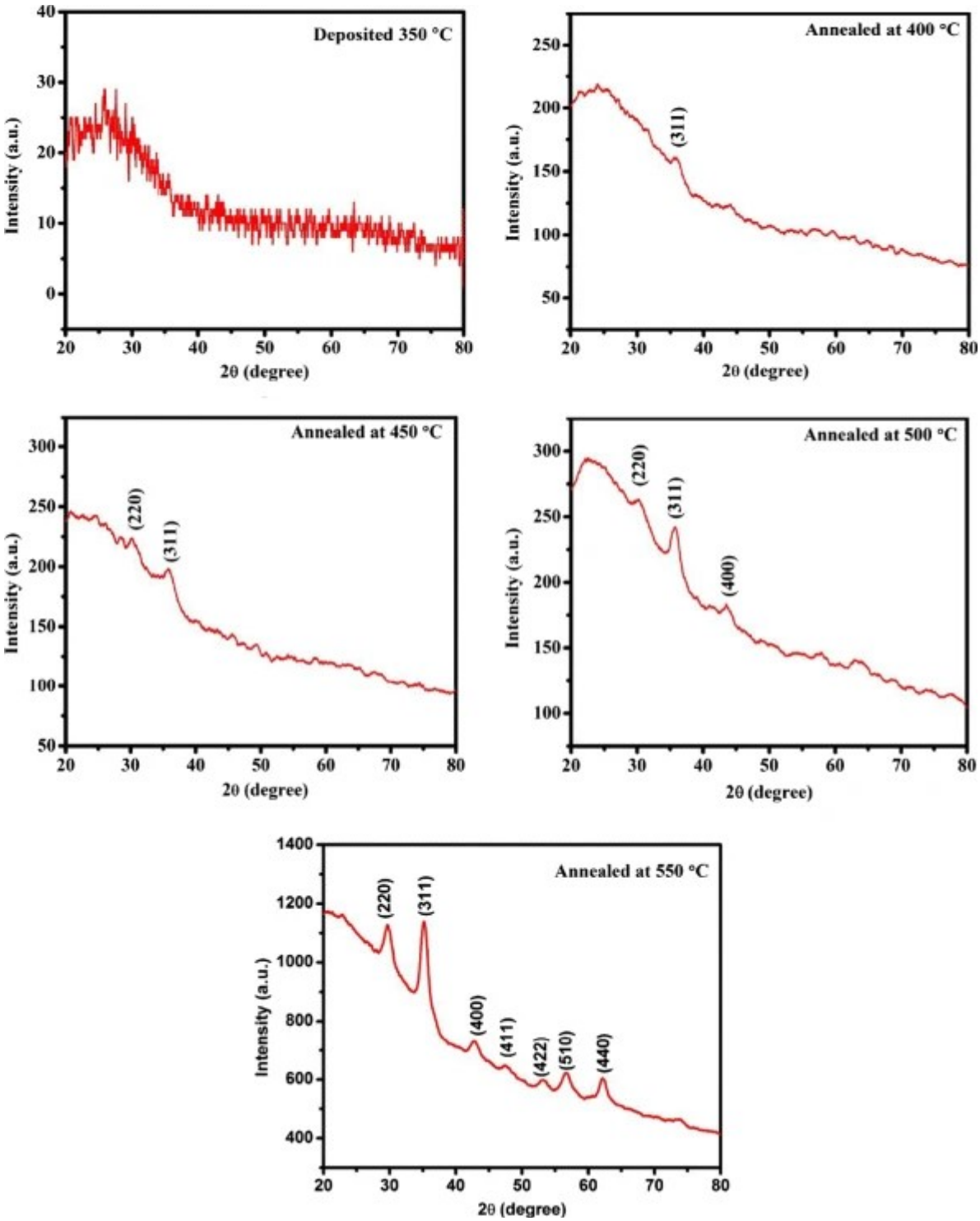

X-ray diffraction at deposited temperature (350 °C) and different annealing temperatures (400, 450, 500 and 550 °C) of $NiFe_2O_4$ thin films

Fig. 2

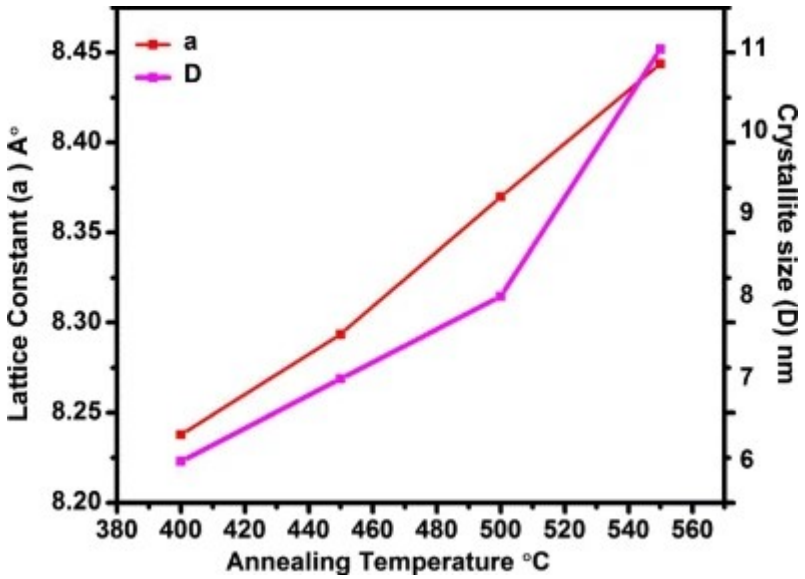

Lattice constant (a) and crystallite size (D) of $NiFe_2O_4$ ferrite thin films with different annealing temperatures

Table 2 Lattice constant (a), X-ray density (d_X) and crystallite size (D) at different annealing temperatures of $NiFe_2O_4$ thin films

3.2 FT-IR Studies

The FT-IR absorption spectra of as-deposited (350 \(^{\circ }\)C) and annealed at 400 and 550 \(^{\circ }\)C $NiFe_2O_4$ thin films in the range of 4000 to 350 cm^{-1} are shown in Fig. 3a–c. It is evident from Fig. 3a that the five sharp absorption bands at υ_1\(=\) 355 cm^{-1}, \(\upsilon _{2}\)\(=\) 616 cm^{-1}, \(\upsilon _{3}\)\(=\) 1042 cm^{-1}, \(\upsilon _{4}\)= 1602 cm^{-1} and \(\upsilon _{5}\)\(=\) 3515 cm^{-1} are observed. These absorption bands are attributed to the stretching vibration of Fe-O, stretching vibration in goethite, O-H deformation vibrations in lepidocrocite and stretching vibration of –OH bond in the hydroxide content, respectively [23]. Due to the metal oxide vibrations, there were two absorption bands: one at 355 cm^{-1} and another at 616 cm^{-1}. These two bands are confirmed at the octahedral and tetrahedral sites of

the spinel structure $NiFe_2O_4$ thin film. This result indicated that the as-deposited thin film contained hydroxide and other bonds. Therefore, after annealing of the as-deposited $NiFe_2O_4$ thin film, the hydroxide bond (υ_9 and \(\upsilon _{13}\)) is reduced at 3483 and 3435 as shown Fig. 3b, c. For an inverse spinel ferrite with one assigned absorption, two bands appeared at 610 and 394 cm^{-1}, which were attributed to the stretching vibration of the tetrahedral group $Fe^{3+}-O^{2-}$. These two strong absorption bands are typical of inverse spinel ferrites, and the positions of these infrared bands are in the range which corresponds to nickel ferrite [27]. Basically, considering the FT-IR spectra, it can be concluded that the spray pyrolysis technique results into the deposition of single-phase cubic spinel nanocrystalline $NiFe_2O_4$ thin films. The authors have shown that there is gradual removal of hydroxyl groups when the annealing temperature is increased.

Fig. 3

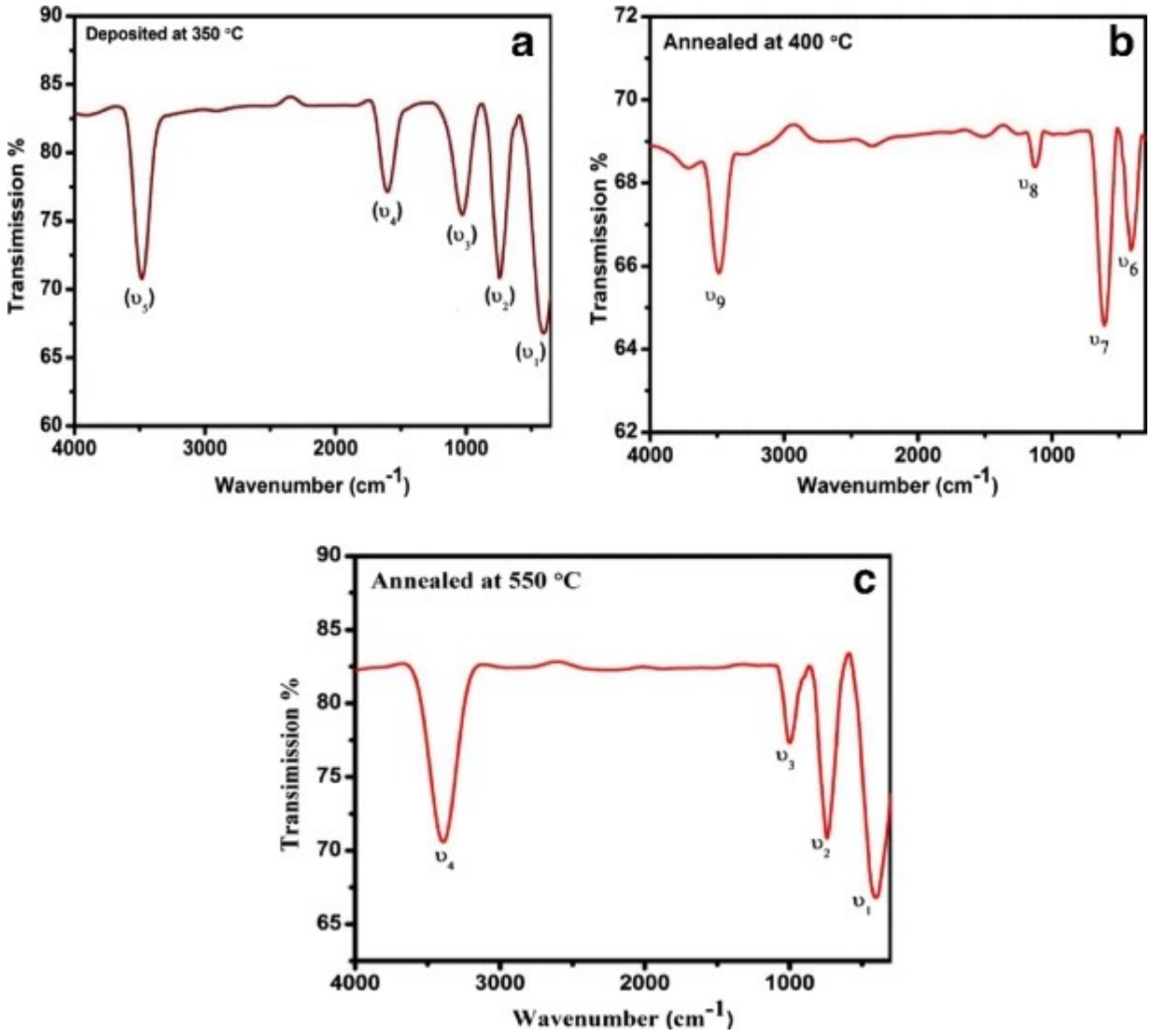

a–c FTIR spectra for typical samples of $NiFe_2O_4$ thin films

3.3 Surface Morphology

The surface morphological studies of the $NiFe_2O_4$ thin films (deposited and differently annealed) have been carried out using field emission scanning electron microscopy (FE-SEM) as shown in Fig. 4a–e. It is clear from the deposited film that the solid spherical grains are uniformly distributed throughout. However, the grains are clustering slightly after being annealed at 400 \(^{\circ }\)C in the film [28]. Films annealed at 450, 500 and 550 \(^{\circ }\)C show the density of enhanced film due to the grains is clearly coalescence. Figure 4d, e shows the microstructural evolution observed during annealing at the temperatures 500 and 550 \(^{\circ }\)C. This sequence of images clearly shows the abnormal grain growth process and the formation growth of twins. It means that the average grain size increases with the increase of annealing temperature as shown in Table 3. Figure 5 shows that the average grain size increases with an increase in annealing temperature. The obtained FE-SEM images clearly indicate well-grown grains, and the observed pattern is a grain-like morphology structure. As also observed, the surface of the films having the uniform nature without any crack as well as more agglomerations is present in samples, and such agglomeration may be due to magnetic ion interaction [29]. In this result, the grain growth can be mainly attributed to increasing atomic mobility on the surface and, finally, a decrease of total energy in the film [30]. The average grain size obtained from slow scan XRD pattern is in good agreement with that from FE-SEM images.

Fig. 4

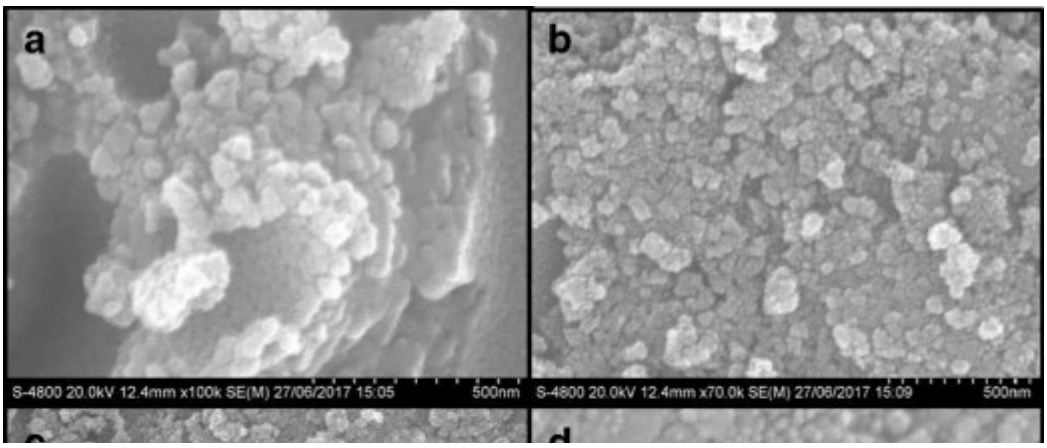

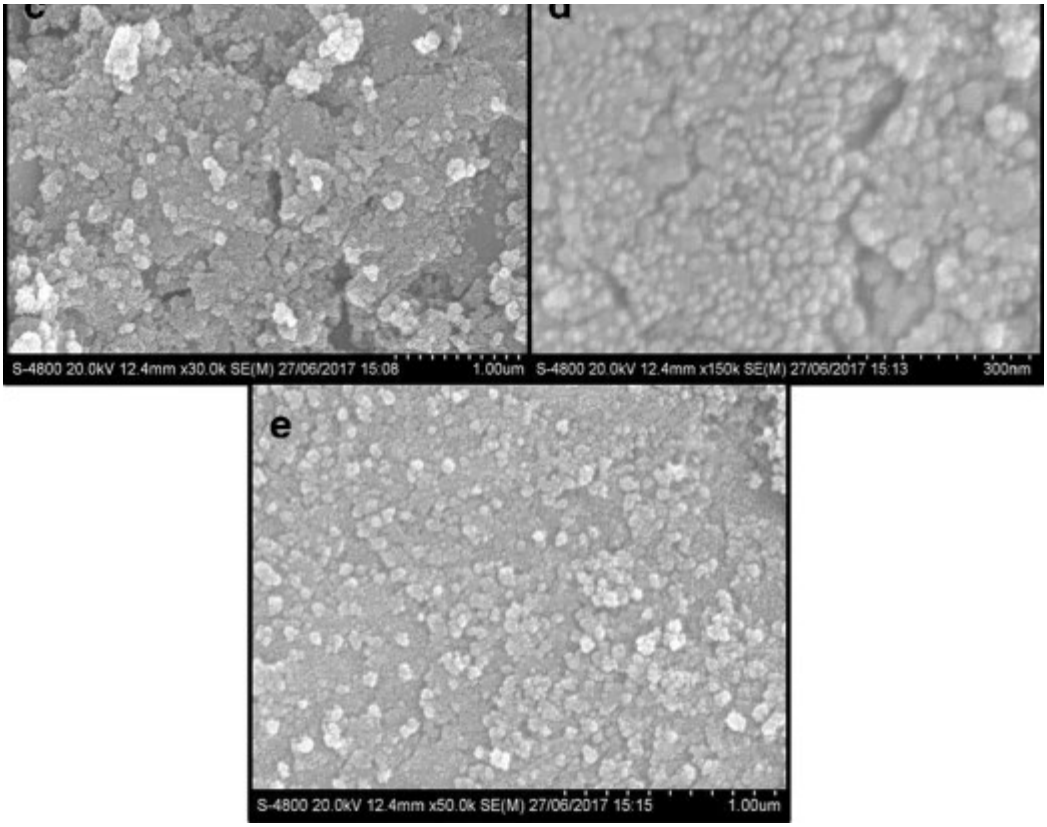

a–e FE-SEM images of the deposited temperature (350 °C) and different annealing temperatures (400, 450, 500 and 550 °C) of $NiFe_2O_4$ thin films

Fig. 5

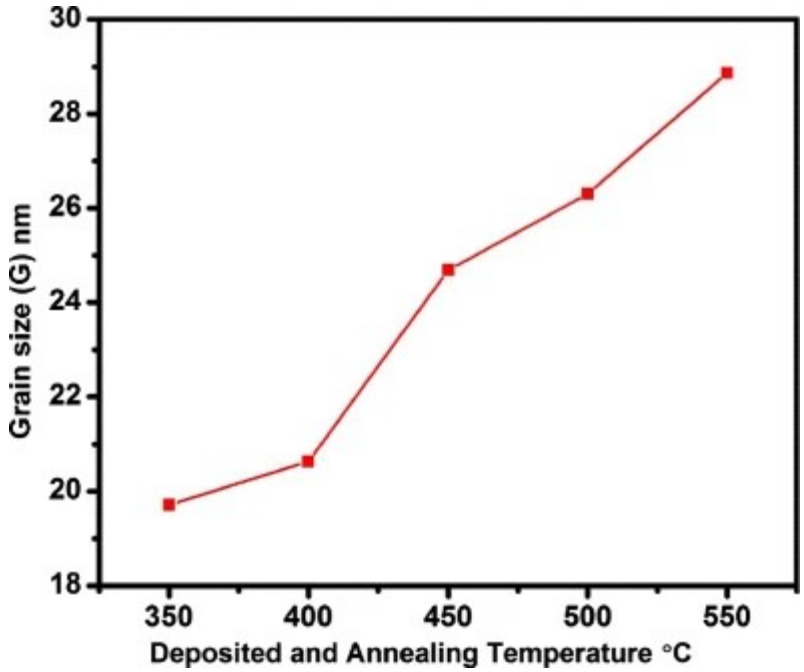

Estimated grain sizes at deposited and different annealing temperatures

Table 3 Energy band gap (E_g) and grain size (G) (deposited and different annealing temperatures) of $NiFe_2O_4$ thin films

3.4 Optical Properties

The optical properties of nickel ferrite (deposited and annealed) thin films on a glass substrate were studied using a UV–vis spectrophotometer. Figure 6 shows that the absorption spectra of nanocrystalline $NiFe_2O_4$ ferrite thin films were recorded at room temperature in the wavelength range of 400–1000 nm by subtracting the absorbance of the glass substrate. Optical absorbance increases with an increase in annealing temperature from 400 to 550 \(^{\circ }\)C until a value of 90% for the films annealing at 550 \(^{\circ }\)C, because of the structural homogeneity, crystallinity and thickness of films [31]. The values of the band gap of the films have been determined from transmission spectra by using the following relation applicable to near-edge optical absorption of semiconductors [16]:

$$ \alpha =\frac{A(hv-E_{\mathrm{g}})^{n/2}}{hv} $$

(3)

where \(\alpha \) is the absorption coefficient, A is the constant independent of \(h\nu \), \(h\nu \) is the photon energy in electron volts, E_g is the band gap and n is a number equal to 1 for the direct band gap and 4 for the indirect gap of $NiFe_2O_4$ thin film. The band gap energy of $NiFe_2O_4$ thin films has been determined by the Tauc plot based on the above formula as shown in Fig. 7a–e. The optical band gaps are found to be 3.26, 3.12, 2.98, 2.83 and 2.75 eV for the films as-deposited and annealed at 440, 450, 500 and 550 \(^{\circ }\)C temperatures, respectively. The band gap of the as-deposited or unannealed film is higher compared to the annealed $NiFe_2O_4$ thin films because the deposited 350 \(^{\circ }\)C temperature gives rise to film with smaller crystallite size [32]. The energy band gap of $NiFe_2O_4$ thin films tends to

decrease as the annealing temperature is increased due to increased crystallite size of the films. Table 3 shows the enrgy band gap and thickness of thin films of deposited and different annealing temperature. The decreases in thickness of thin films at increasing annealing temperatures (550 \(^{\circ }\)C) may be due to the evaporation of the solution and, previously, to the substrate causing, in ferric, a less amount of residue reaching the glass substrates. The result decreases the thickness of the films at higher temperature. Also, thermophoretic force at higher annealing temperature (550 \(^{\circ }\)C) is higher and it repels the aerosol droplets causing a decrease in thickness as reported earlier [33].

Fig. 6

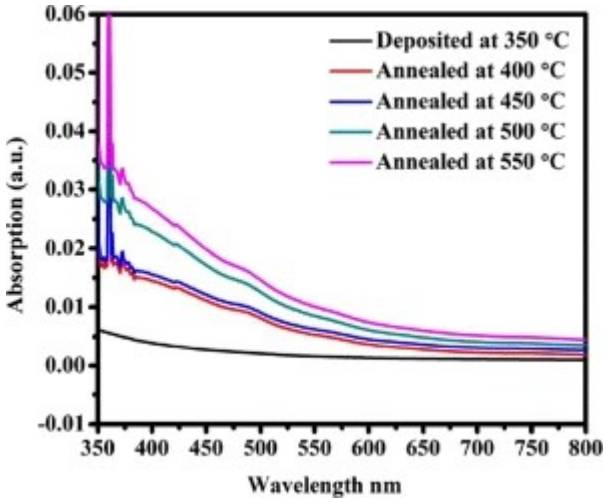

UV-visible absorbance spectra of the deposited temperature (350 °C) and different annealing temperatures (400, 450, 500 and 550 °C) of $NiFe_2O_4$ thin films

Fig. 7

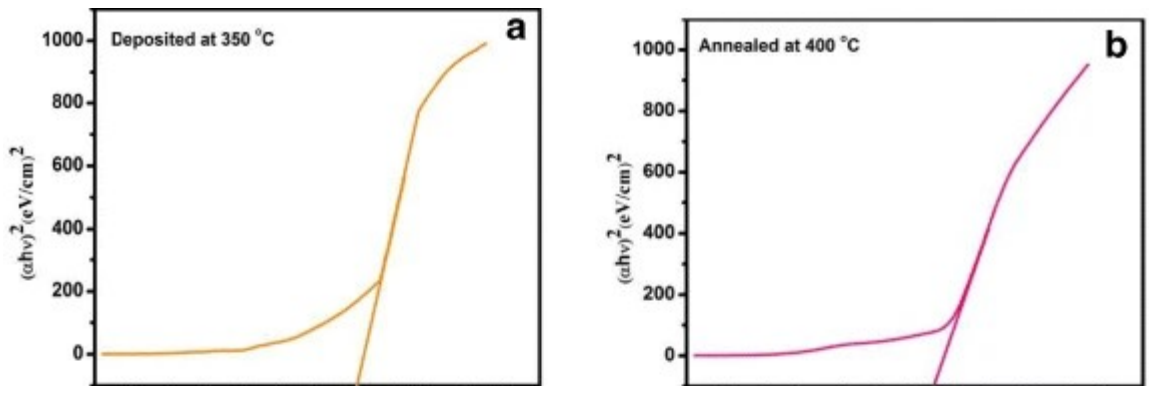

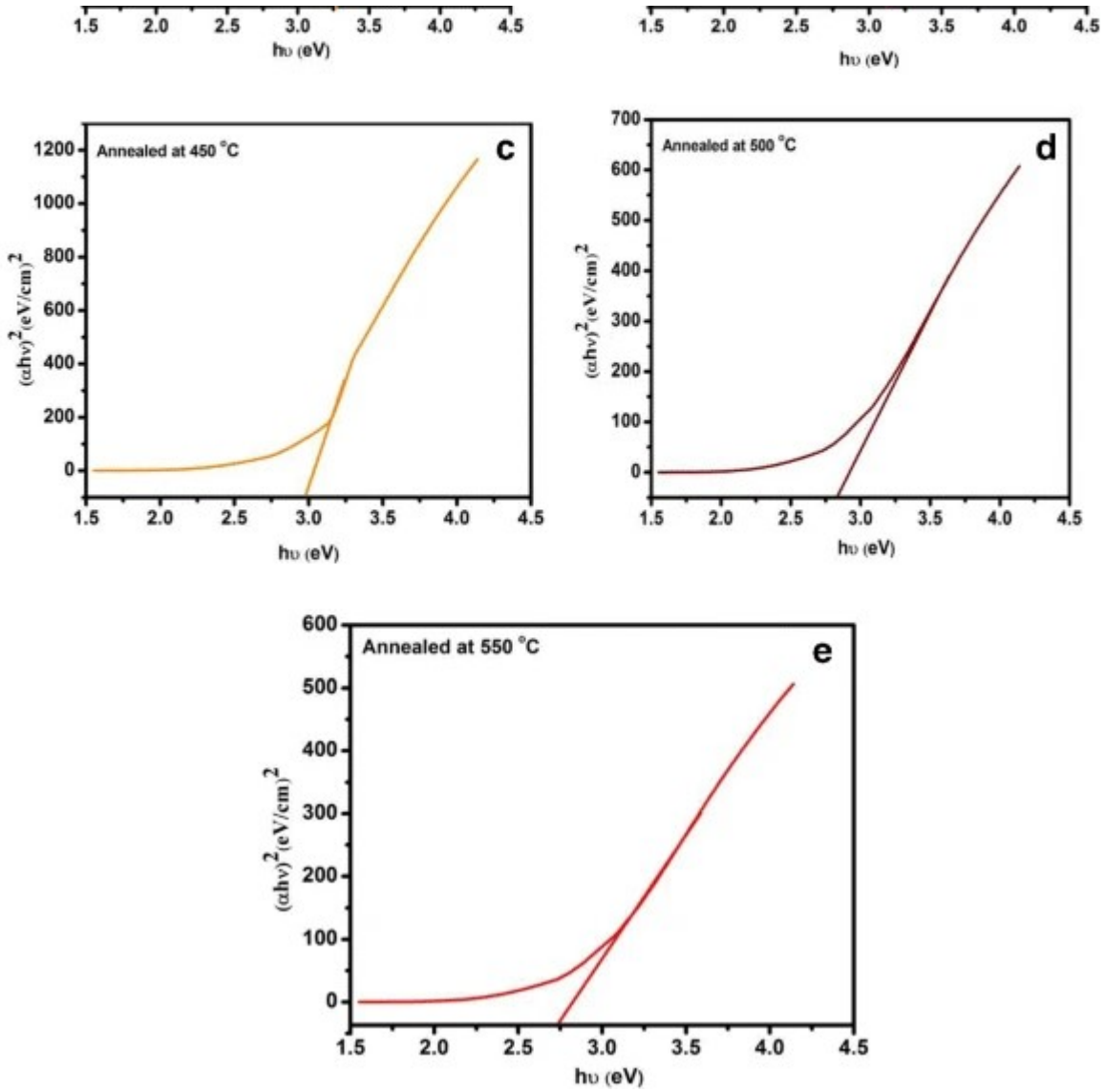

a–e The energy band gap at the deposited temperature (350 °C) and different annealing temperatures (400, 450, 500 and 550 °C) of $NiFe_2O_4$ thin films

3.5 Magnetic Properties

The magnetic measurements on the $NiFe_2O_4$ thin film sample deposited at the temperature 350 \(^{\circ }\)C and typically annealing temperatures 450 and 550 \(^{\circ }\)C were performed using a vibrating sample magnetometer (VSM) at room temperature. Figures 8 and 9 show that all the samples are clearly in magnetic hysteresis loop, which reveal that they have a good ferrimagnetism property and it confirms that the desired $NiFe_2O_4$ thin films were successfully obtained. The experimental magnetic moment values (η_B) in Bohr magnetons are calculated by using the following formula [34]:

$$ \eta_{\mathrm{B}} =\frac{M_{\mathrm{w}} \times M_{\mathrm{s}}}{5585} $$

(4)

Fig. 8

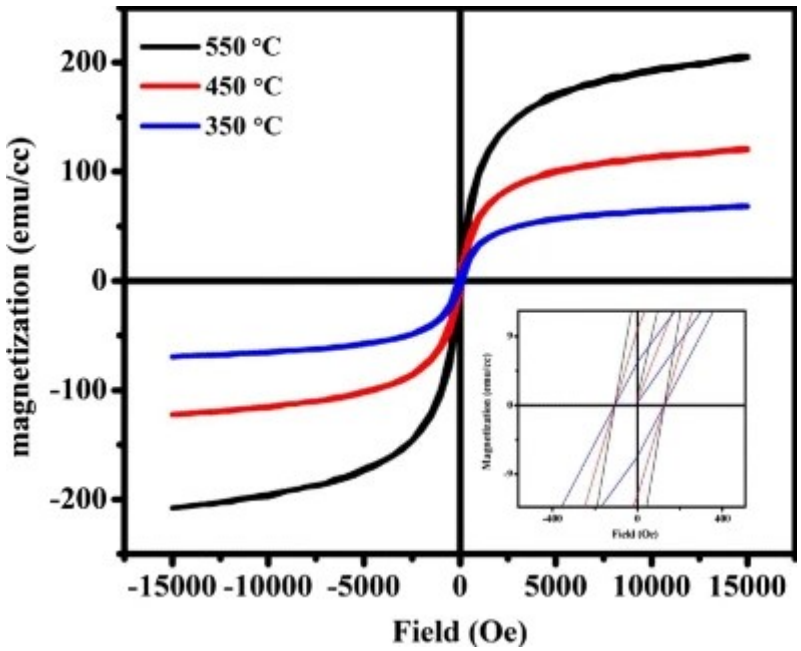

Magnetic hysteresis loops of $NiFe_2O_4$ thin films at the deposited temperature (350 °C) and annealed temperatures (450 and550 °C)

Fig. 9

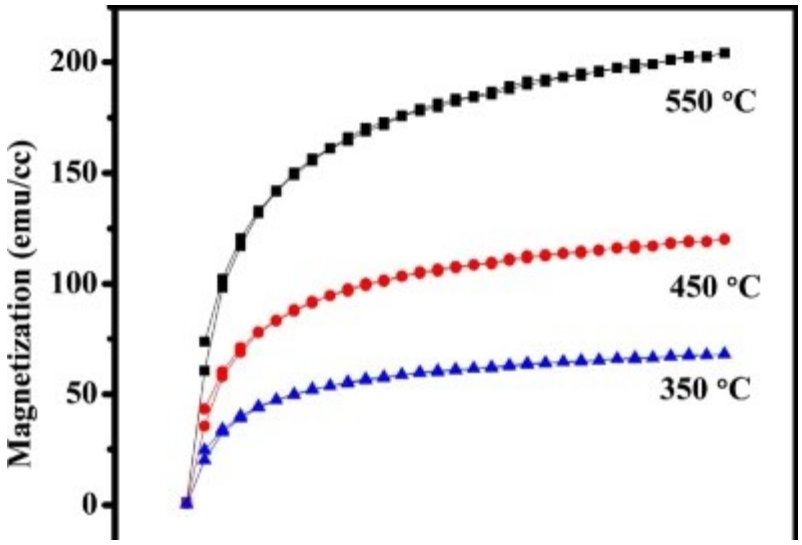

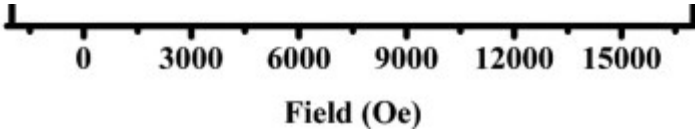

M–H curves of $NiFe_2O_4$ thin films at the deposited temperature (350 °C) and annealed temperatures (450 and 550 °C)

where \(M_{\mathrm {w}}\) is the molecular weight and \(M_{\mathrm {s}}\) is the saturation magnetization (emu/cm^3) of the thin film sample, respectively. The magnetic parameters of the sample, such as saturation magnetization (M_s), coercivity field (H_c), remanence (M_r) and experimental Bohr magnetons (η_B), with different annealing temperatures are summarized in Table 4. The saturation magnetization of as-deposited film at the temperature 350 °C is found to be 68.29 emu/cm^3, and after being annealed at 450 and 550 \(^{\circ }\)C temperatures, the values are found to be in the range 119.34 to 205.51 emu/cm^3 [35]. It reveals that the saturation magnetization (M_s) of films increased drastically while coercivity (H_c) steadily increases with the annealing temperature. The lower value of \(M_{\mathrm {s}}\) for the as-deposited thin film may be due to the partial crystallization structure of the sample. Another reason for the increase in \(M_{\mathrm {s}}\) for annealed thin film samples can be well explained on the basis of spinel structure and the enhancement in crystallinity after annealing. The effect of annealing temperature on the saturation magnetization could also be attributed to cation distribution and crystallinity of the films [36]. The $NiFe_2O_4$ thin films obtained a perfect cation distribution due to their inverse spinel structure. In the high annealing temperature, the cations can maximum diffusion energy to a potential barrier in order to reach an ideal position and also obtained high saturation magnetization. The higher annealing effect of $NiFe_2O_4$ films is probably due to better crystallinity and the transformation of super-paramagnetic or non-magnetic amorphous phase to the ferromagnetic spinel phase [37]. It means that the improvement of crystallinity increases the particles size but decreases the concentration of oxygen vacancies and strengthening of the Fe^{3+}–O^{2}–Fe^{3-} exchange interaction. However, the result of coercivity can be well explained by the difference of the grain size under different annealing temperatures from SEM analysis [38]. As per the concern of exchange coupling theory for nanocrystalline ferromagnetic materials, an increase in grain size results to an increase in the

coercivity. According to the reported literature, the coercivity of nickel ferrite thin films get improved due to an increase in annealing temperature [39]. In the present investigation, the coercivity increases with a gradual increase in grain size as annealing temperature increases.

Table 4 Saturation magnetization (M_s), remanence (M_r), coercivity (H_c), calculated Bohr magnetrons \(\eta _{\mathrm {B}}(\mu _{\mathrm {B}})\) and observed Bohr magnetrons \(\eta _{\mathrm {B}}(\mu _{\mathrm {B}})\) of $NiFe_2O_4$ thin films estimated from VSM analysis

4 Conclusions

The nickel ferrite thin films have been successfully deposited on glass substrates by using a spray pyrolysis technique. The process of deposited temperature and annealing in the air has been found to change the crystallinity of films from oriented nanocrystalline cubic spinel structure for XRD analysis. It was observed that the as-deposited film has an amorphous-like structure and has relatively low \(H_{\mathrm {c}}\) and \(M_{\mathrm {s}}\) values. After these films were annealed at different temperatures with crystallization peak, the crystallinity is enhanced and the \(H_{\mathrm {c}}\) and \(M_{\mathrm {s}}\) values are significantly increased. The FT-IR spectra of $NiFe_2O_4$ thin films showed strong absorption peaks around 630 and 350 cm^{-1}, indicating the characteristic feature of spinel ferrite. The nanocrystalline grains increase, and the number of distinct microcrystal develops on top of the film surface. The crystals grow to a maximum size at 550 \(^{\circ }\)C, having clear crystallographic faces on their surface. The energy band gap decreases from 3.26 to 2.75 eV for the as-deposited and annealed $NiFe_2O_4$ thin films. Together with the annealing temperature, the spray pyrolysis method becomes a convenient method for preparation of nickel ferrite thin films.

References

1. Ray, N. M.: Synthesis and Characterization of Nanocrystalline Nickel-Zinc Spinel Ferrite Thin Films Using the Spin-Spray Deposition Method. Arizona State University (2013)

2. Rani, N., Sharma, P.G.: Magnetic studies on $CoFe_2O_4$ thin films prepared by spin coating method (2017)

3. Maensiri, S., Masingboon, C., Boonchom, B., Seraphin, S.: A simple route to synthesize nickel ferrite ($NiFe_2O_4$) nanoparticles using egg white. Scripta Mater. 56(9), 797–800 (2007)

Article Google Scholar

4. Raghasudha, M., Ravinder, D., Veerasomaiah, P.: Characterization of chromium substituted cobalt nano ferrites synthesized by citrate-gel auto combustion method. Adv. Mater. Phys. Chem. 3(2), 89 (2013)

Article Google Scholar

5. Morega, A., Morega, M., Pîslaru-Dănescu, L., Stoica, V., Nouraş, F., Stoian, F.D.: A novel, ferrofluid-cooled transformer. In: 2010 12th International Conference on Electromagnetic Field and Heat Transfer by Numerical Simulation, Optimization of Electrical and Electronic Equipment (OPTIM), pp. 140–146. IEEE (2010)

6. Joseph, J., Tangsali, R., Pillai, V. M., Choudhary, R., Phase, D., Ganeshan, V.: Structure and magnetic properties of highly textured nanocrystalline Mn–Zn ferrite thin film. Physica B: Cond. Matter 456, 293–297 (2015)

Article ADS Google Scholar

7. Arabi, H., Moghadam, N. K.: Nanostructure and magnetic properties of magnesium ferrite thin films deposited on glass substrate by spray pyrolysis. J. Magn. Magn. Mater. 335, 144–

148 (2013)

Article ADS Google Scholar

8. Ahmad, Z., Atiq, S., Abbas, S. K., Ramay, S. M., Riaz, S., Naseem, S.: Structural and complex impedance spectroscopic studies of Mg-substituted $CoFe_2O_4$. Cer. Intern. 42(16), 18271–18282 (2016)

Article Google Scholar

9. Panwar, K., Tiwari, S., Bapna, K., Heda, N., Choudhary, R., Phase, D., Ahuja, B.: The effect of Cr substitution on the structural, electronic and magnetic properties of pulsed laser deposited $NiFe_2O_4$ thin films. J. Magn. Magn. Mater. 421, 25–30 (2017)

Article ADS Google Scholar

10. Beji, Z., Smiri, L., Yaacoub, N., Greneche, J. -M., Menguy, N., Ammar, S., Fiévet, F.: Annealing effect on the magnetic properties of polyol-made Ni–Zn ferrite nanoparticles. Chem. Mater. 22(4), 1350–1366 (2010)

Article Google Scholar

11. Shirsath, S. E., Toksha, B., Jadhav, K.: Structural and magnetic properties of In 3 + substituted $NiFe_2O_4$. Mater. Chem. Phys. 117(1), 163–168 (2009)

Article Google Scholar

12. Bellad, S., Bhosale, C.: Substrate temperature dependent properties of sprayed $CoFe_2O_4$ ferrite thin films. Thin Solid Films 322(1), 93–97 (1998)

Article ADS Google Scholar

13. Darshane, S. L., Suryavanshi, S., Mulla, I.: Nanostructured nickel ferrite: a liquid petroleum gas sensor. Cer. Intern. 35(5), 1793–1797 (2009)

Article Google Scholar

14. Anjum, S., Jaffari, G.H., Rumaiz, A.K., Rafique, M.S., Shah, S.I.: Role of vacancies in transport and magnetic properties of nickel ferrite thin films. J. Phys. D: Appl. Phys. 43(26), 265001 (2010)

Article ADS Google Scholar

15. Liang, Y. -C., Hsia, H. -Y.: Growth and crystallographic feature-dependent characterization of spinel zinc ferrite thin films by RF sputtering. Nanoscale Res. Lett. 8(1), 537 (2013)

Article ADS Google Scholar

16. Chavan, S., Babrekar, M., More, S., Jadhav, K.: Structural and optical properties of nanocrystalline Ni–Zn ferrite thin films. J. Alloys Compd. 507(1), 21–25 (2010)

Article Google Scholar

17. Sedlář, M., Matějec, V., Grygar, T., Kadlecová, J.: Sol–gel processing and magnetic properties of nickel zinc ferrite thick films. Cer. Intern. 26(5), 507–512 (2000)

Article Google Scholar

18. NuLi, Y. -N., Qin, Q. -Z.: Nanocrystalline transition metal ferrite thin films prepared by an electrochemical route for Li-ion batteries. J. Power Sources 142(1), 292–297 (2005)

Article ADS Google Scholar

19. Kumbhar, S., Mahadik, M., Mohite, V., Rajpure, K., Bhosale, C.: Synthesis and characterization of spray deposited nickel-zinc ferrite thin films. Energy Procedia 54, 599–605 (2014)

Article Google Scholar

20. Ray, S. C.: Preparation of copper oxide thin film by the sol–gel-like dip technique and study of their structural and optical properties. Sol. Energy Mater. Sol. Cells 68(3), 307–312 (2001)

Article Google Scholar

21. Elangovan, E., Singh, M., Ramamurthi, K.: Studies on structural and electrical properties of spray deposited SnO_2: F thin films as a function of film thickness. Mater. Sci. Eng.: B 113(2), 143–148 (2004)

Article Google Scholar

22. Dixit, G., Singh, J. P., Srivastava, R., Agrawal, H., Choudhary, R., Gupta, A.: Annealing effect on the structural and magnetic properties of nickel ferrite thin films. Surf. Interface Anal. 42(3), 151–156 (2010)

Article Google Scholar

23. Gunjakar, J., More, A., Gurav, K., Lokhande, C.: Chemical synthesis of spinel nickel ferrite ($NiFe_2O_4$) nano-sheets. Appl. Surf. Sci. 254(18), 5844–5848 (2008)

Article ADS Google Scholar

24. Kumbhar, S., Mahadik, M., Mohite, V., Hunge, Y., Rajpure, K., Bhosale, C.: Effect of Ni content on the structural, morphological and magnetic properties of spray deposited Ni–Zn ferrite thin films. Mater. Res. Bull. 67, 47–54 (2015)

Article Google Scholar

25. Khirade, P. P., Birajdar, S. D., Raut, A., Jadhav, K.: Multiferroic iron doped $BaTiO_3$ nanoceramics synthesized by sol-gel auto combustion: influence of iron on physical properties. Cer. Intern. 42(10), 12441–12451 (2016)

Article Google Scholar

26. Hankare, P., Patil, R., Garadkar, K., Sasikala, R., Chougule, B.: Synthesis, dielectric behavior and impedance measurement studies of Cr-substituted Zn–Mn ferrites. Mater. Res. Bull. 46(3), 447–452 (2011)

Article Google Scholar

27. Kapse, V., Ghosh, S., Raghuwanshi, F., Kapse, S., Khandekar, U.: Nanocrystalline $Ni_{0.6}Zn_{0.4}Fe_2$ O $_4$: A novel semiconducting material for ethanol detection. Talanta 78(1), 19–25 (2009)

Article Google Scholar

28. Kim, D. -H., Lee, S. -H., Kim, J. -K., Lee, G. -H.: Structure and electrical transport properties of bismuth thin films prepared by RF magnetron sputtering. Appl. Surf. Sci. 252(10), 3525–3531 (2006)

Article ADS Google Scholar

29. Chavan, A. R., Birajdar, S. D., Chilwar, R. R., Jadhav, K.: Structural, morphological, optical, magnetic and electrical properties of Al 3 + substituted nickel ferrite thin films. J. Alloys Compd. (2017)

30. Farkas, D., Mohanty, S., Monk, J.: Linear grain growth kinetics and rotation in

nanocrystalline. Ni. Phys. Rev. Lett. 98(16), 165502 (2007)

Article ADS Google Scholar

31. Venzke, S., Van Dover, R., Phillips, J. M., Gyorgy, E., Siegrist, T., Chen, C., Werder, D., Fleming, R., Felder, R., Coleman, E.: Epitaxial growth and magnetic behavior of $NiFe_2O_4$ thin films. J. Mater. Res. 11(5), 1187–1198 (1996)

Article ADS Google Scholar

32. Sutka, A., Strikis, G., Mezinskis, G., Lusis, A., Zavickis, J., Kleperis, J., Jakovlevs, D.: Properties of Ni–Zn ferrite thin films deposited using spray pyrolysis. Thin Solid Films 526, 65–69 (2012)

Article ADS Google Scholar

33. Palgrave, R.: Chemical Vapour Deposition of Nanoparticulate and Nanocomposite Thin Films. University of London University College London (United Kingdom) (2007)

34. Jadhav, J., Biswas, S., Yadav, A., Jha, S., Bhattacharyya, D.: Structural and magnetic properties of nanocrystalline Ni Zn ferrites: in the context of cationic distribution. J. Alloys Compd. 696, 28–41 (2017)

Article Google Scholar

35. Phua, L., Xu, F., Ma, Y., Ong, C.: Structure and magnetic characterizations of cobalt ferrite films prepared by spray pyrolysis. Thin Solid Films 517(20), 5858–5861 (2009)

Article ADS Google Scholar

36. Wang, L., Nie, S., Wang, J., Xu, L., Yuan, B., Liu, X., Luo, Q., Chen, Y., Yue, G., Peng, D.: Effect of experiment parameters on the structure and magnetic properties of NiZn-

ferrite films. Mater. Chem. Phys. 160, 321–328 (2015)

Article Google Scholar

37. Dash, J., Prasad, S., Venkataramani, N., Krishnan, R., Kishan, P., Kumar, N., Kulkarni, S., Date, S.: Study of magnetization and crystallization in sputter deposited LiZn ferrite thin films. J. Appl. Phys. 86(6), 3303–3311 (1999)

Article ADS Google Scholar

38. Singh, R., Narayan, A., Prasad, K., Yadav, R., Pandey, A., Singh, A., Verma, L., Verma, R.: Thermal, structural, magnetic and photoluminescence studies on cobalt ferrite nanoparticles obtained by citrate precursor method. J. Therm. Anal. Calorim 110(2), 573–580 (2012)

Article Google Scholar

39. Gupta, N., Verma, A., Kashyap, S. C., Dube, D.: Microstructural, dielectric and magnetic behavior of spin-deposited nanocrystalline nickel–zinc ferrite thin films for microwave applications. J. Magn. Magn. Mater. 308 (1), 137–142 (2007)

Article ADS Google Scholar

Acknowledgements

The author (A. R. Chavan) is thankful to the Solapur University, Solapur; North Maharashtra University, Jalgaon; and IIT, Madras, for providing the XRD, FE-SEM and VSM characterization facility.

Author information

Authors and Affiliations

Department of Physics, Dr. Babasaheb Ambedkar Marathwada University, Aurangabad, Maharashtra, 431004, India
Apparao R. Chavan, Prashant B. Kharat & K. M. Jadhav

Department of Physics, Yogeshwari College Ambajogai, Beed, Maharashtra, 431517, India
Rahul R. Chilwar

Corresponding author

Correspondence to K. M. Jadhav.

Rights and permissions

About this article

Cite this article

Chavan, A.R., Chilwar, R.R., Kharat, P.B. *et al.* Effect of Annealing Temperature on Structural, Morphological, Optical and Magnetic Properties of $NiFe_2O_4$ Thin Films. *J Supercond Nov Magn* 31, 2949–2958 (2018). https://doi.org/10.1007/s10948-018-4565-3

Received	Accepted	Published
01 January 2018	08 January 2018	18 January 2018

Issue Date
September 2018

DOI
https://doi.org/10.1007/s10948-018-4565-3

Share this article

Anyone you share the following link with will be able to read this content:

Get shareable link

Keywords

Nickel ferrite Annealing temperature XRD FT-IR FE-SEM UV-vis VSM